ORIGINAL PAPER

Bio-based hybrid cabin door of ultralight helicopter with variable-axis fiber design

Rostislav Svidler[1] · R. Rinberg[1]

Abstract

This paper presents the development of an integrated technology concept for the production of semi-structural fiber composite aerospace components with a bio-based hybrid laminate structure. In this context, the high lightweight potential of a variable-axial hybrid fiber-reinforced laminates compared to a multiaxial laminate design is of particular importance. As a demonstrator, a double-shell cabin door based on the cabin door of the ultra-light helicopter CoAx 2D of EDM Aerotec GmbH was redesigned in hybrid bio-based mixed composite construction using selected finite-element method (FEM) simulation and optimization tools, manufactured and characterized. The obtained results illustrate that compared to the reference carbon fiber-reinforced polymer (CFRP) component, the developed bio-based hybrid composite with local tailored fiber placement (TFP) reinforcement has a 30% biomass content, exhibits comparable mechanical properties and significantly contributes to increase energy and resource efficiency significantly.

Keywords Fiber-reinforced polymer · CFRP · Bio-based fiber composites · Flax fiber composite · Tailored fiber placement · TFP · Finite-element method · FEM

List of symbols

vol.%	Volume percent
wt%	Mass percent

Abbreviations

FEM	Finite-element method
FRP	Fibre-reinforced plastics
CFRP	Carbon fiber-reinforced plastics
FFRP	Flax fiber-reinforced plastics
TFP	Tailored fiber placement
CF	Carbon fiber
FF	Flax fiber
GF	Glass fiber
ULH	Ultra-light helicopter
UD	Unidirectional
BD	Bidirectional
UHM	Ultra high modulus
UHT	Ultra high strength
ULH	Ultra-light helicopter
EP	Epoxy

RTM	Resin transfer moulding
VARI	Vacuum assisted resin infusion
aVARI	Autoclave supported VARI

✉ Rostislav Svidler
rostislav.svidler@mb.tu-chemnitz.de

1 Department of Lightweight Structures and Polymer Technology, Chemnitz University of Technology, 09107 Chemnitz, Germany

1 Introduction

One of the common solutions for achieving a high lightweight degree in aircraft and helicopter construction is the substitution of light metal aerospace materials, such as aluminium or titanium, by fiber-reinforced plastic composites (FRP) made of glass, carbon or aramid fibers. The production of FRP structures requires a high input of resources; in addition, the recycling of old components is a major challenge. This has a negative impact on recycling costs and the overall carbon footprint of the aircraft structure [1]. To increase the eco-efficiency of flying, bio-based fiber composites can be used to minimize the final product's environmental impact. So far, highly stressed aerospace components have not yet been implemented from natural fiber-based lightweight materials due to the fact that its mechanical properties are significantly lower than those of CFRP. This means that pure material substitution is rarely a practical option.

A promising solution to meet the aerospace requirements is the hybridisation of natural fiber-based FRP,

which implies a tailored integration of carbon fibers in the direction of the application critical stresses present in the component. For such hybridization, variable-axis fiber deposition methods (e.g., TFP) or smart hybrid multiaxial laminate design can be used [2, 3]. The use of TFP reinforcements requires the development of a holistic technological approach for the numerical design as well as FEM-based simulation of hybrid composites using modern topology and material optimization techniques, with sufficient consideration of manufacturing aspects [4, 5].

This work provides an insight into the performed design of a cabin door of an ultra-light helicopter (ULH) in hybrid design with a partial TFP reinforcement as well as into the development of an integrated technology concept. It is based on an interactive solution approach for the simultaneous development of optimum material composites, manufacturing processes and integrative construction methods. Although there have been similar works in the past [6], the focus of the research there was on geometry optimization and the presentation of a general viability under integration of partial UD-CFRP patches into the flax fiber composite. The patch geometry was defined empirically based on the main stress vectors. The work [6] can be considered as a preliminary stage, but the main difference lies in the unified analytical solution approach, where the design is primarily based on the FEM results. Such a solution approach has barely been pursued so far for sustainable, bio-based aerospace structures.

2 Materials

For the work carried out on the design of the hybrid helicopter door, commercially available materials were selected and processed into thermoset fiber composite panels and test specimens. To determine the required characteristic values, mechanical tests were carried out in compliance with DIN EN ISO 527-5, EN ISO 14129 and DIN EN ISO 14126. Other important characteristic values were partly taken from data sheets and literature or assumed on the basis of empirical values.

2.1 Polymer matrices

To increase the biogenic content of the hybrid composite, a 19 wt% bio-based thermosetting epoxy resin SuperSap INR/INS (EntropyResins) was used as matrix material in the work. This EP system has a viscosity B of 25 cPs at 25 °C as well as a pot life of 180 min and can be processed by VARI or RTM.

2.2 Carbon fibers

The CF semi-finished products used were a UD scrim of the type ZOLTEK PX 35 with a basis weight of 150 g/m^2 and a 2/2 twill fabric of the type Style 462 Aero with a basis weight of 250 g/m^2, which are approved for aviation applications. In the autoclave supported vacuum assisted resin injection process (aVARI), a fiber mass fraction of 55–60 wt% can be assumed, which corresponds to a fiber volume fraction of approx. 45 vol.%.

For TFP production high-strength CF rovings with 200 tex (3 K) to 800 tex (12 K) (Carbon-Werke GmbH) were used. To improve fiber–matrix adhesion, these are coated with an epoxy resin (EP) finish (1.5 wt%).

2.3 Flax fibers

Two unidirectional flax fiber fabrics (FF-UD) FlaxTape 110 and UD FAW 150 (quasi-UD fabrics) and a 2/2 twill fabric BD FAW 150 from EcoTechnilin were used as biogenic reinforcement material for the hybrid helicopter door. The numbers in the material designation represent the grammage in g/m^2.

Compared with CF and GF semi-finished products, the FF semi-finished products have some quality deficits with regard to fiber orientation and homogeneity of fiber distribution. This inevitably leads to a higher statistical characteristic value scatter in the test laminates. Furthermore, the fiber volume fractions can be achieved are significantly below those of CF or GF semi-finished products.

3 Manufacturing process

3.1 Tailored fiber placement

Washable paper or thin polyester fleece is often used as embroidery base for TFP production. Textile semi-finished products can also be embroidered directly, thus simplifying the subsequent handling and precise positioning of the local TFP reinforcements. An embroidery machine from TAJIMA was used as the TFP system, with which the CF rovings can be processed up to 24 K. However, very stiff HM-CF or UHM-CF types of are not suitable for process-reliable depositing of embroidery patterns with small radii. Therefore, 3 K, 6 K and 12 K HT-CF rovings were used. A 10 tex polyester thread was used as the embroidery thread. The stitch width (*R* value)—a measure of the bundling or spreading of the roving—and the roving spacing value l_s are determinant parameters in TFP processing [5] and were extensively investigated here. To determine the optimum

embroidery parameters, a quasi-isotropic polyester nonwoven (50 g/m^2) was first used as the embroidery base. Later, the determined embroidery parameters with necessary corrections were transferred to the bio-based semi-finished products BD FAW 150 and UD FAW 150.

The TFP embroidery of uni/bi-directional FF semi-finished products showed significant differences compared to polyester nonwovens. Due to the stretching of the bio-based embroidery base in the stent frame, the R values determined with polyester nonwovens had to be increased by 0.2 mm and l_s had to be decreased by 0.2 mm. The flax fiber fabric BD FAW 150 could be embroidered well both parallel to the fiber and at dent angles. By reducing the embroidery spacing, it was possible to almost completely eliminate fiber endulation on BD FAW 150, especially with 12 CF rovings. In contrast, considerable processing problems were observed with the flax fabric UD FAW 150. As can be seen in Fig. 1, numerous voids occurred both in the deposited CF reinforcement and in the embroidery base due to the embroidery thread tension. Therefore, BD FAW 150 was favored for later investigations. Parameters with necessary corrections were transferred to the bio-based semi-finished products BD FAW 150 and UD FAW 150.

3.2 Specimen and component manufacturing

The autoclave assisted vacuum infusion process (aVARI) was used for specimen and component production. Using an autoclave (min. 5 bar overpressure), the laminate can be compressed more, which leads to higher fiber volume fractions and better mechanical properties even for natural fiber composites. A further advantage is the use of a bio-based thermosetting EP system. In aVARI, as in VARI processes, dry, ready-cut semi-finished reinforcements are placed in a laminating mould according to the laminate build-up plan, sealed airtight with a vacuum film and vacuum impregnated with the matrix resin at room temperature. In the autoclave,
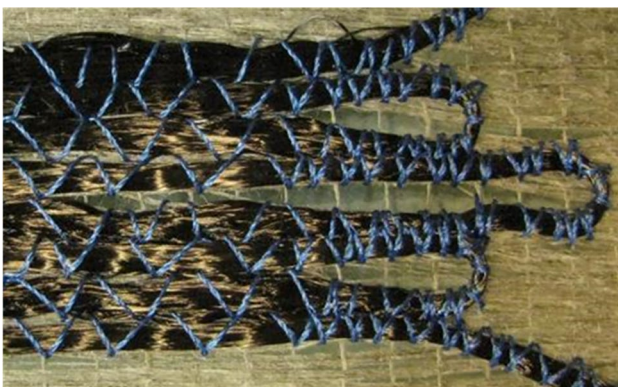
Fig. 1 Manufacturing defects in the TFP of the CF roving on the UD FAW 150 embroidery base

the excess resin is then pressed out by the overpressure and the curing cycle is completed. In this way, fiber contents of up to 50% by volume, which are otherwise normal for prepregs, can be achieved in natural fiber laminates. Compared to prepreg processing, however, the manual production effort is very high.

3.3 Characteristic values for the FEM simulation

To determine the mechanical properties, UD composites and flat TFP semi-finished products were manufactured and consolidated in the VARI process with SuperSap INR/INS to form a symmetrical two-ply UD laminate. Standardized tensile specimens were taken from the laminates by waterjet cutting according to DIN ISO 527-5 and subjected to tensile testing.

Table 1 illustrates the mechanical parameters used for FE-based design, calculation and optimisation. Tensile-based characteristic values were determined experimentally. The pressure-based characteristic values were taken from technical data sheets and/or literature [7–10] or assumed on the basis of empirical values. Fiber volume content was determined gravimetrically. Until all necessary characteristic values are verified by an experimental investigation, a deviation between the simulated and experimental results must be accept.

Specifically, the TFP–FFRP semi-finished product with 12 K CF roving (last column in Table 1) achieved parallel to the fiber a Young's modulus of 47.5 GPa, a tensile strength at break of 738.0 MPa and an elongation at break of 1.5%. Transverse to the fiber is a Young's modulus of 8.7 GPa, tensile strength of 103.8 MPa, and elongation at break of 1.9%. In the parallel fiber direction, these values are well below a CF-UD laminate and slightly above a CF-BD laminate currently used for cabin door production.

In the case of consolidated TFP composite laminates, dry spots were observed between individual CF fiber bundles and, as a result, rough and visually unappealing surfaces. Furthermore, the embroidery thread was clearly visible. In the component design, the TFP reinforcement was not placed in the outer laminate layer or on the visible side of the component to improve the appearance of the component.

4 FEM simulation and optimization

The use of TFP reinforcements requires a detailed understanding of the existing stress state (principal stress distribution) under different load scenarios to design and dimension the component in a stress/production-oriented manner. To get one step closer to this goal, a CAD model of the left cabin door of the UHL CoAx2D was created and the deformation was simulated in Ansys Workbench 19.2 with an

Table 1 Characteristic values used for the FEM simulations

Parameters (unit)	Lineo FlaxTape 110/(INR/INS)	Lineo FlaxPly BD FAW 150 (INR/INS)	CFK-UD ZOLTEKTM PX 35	CFK BD Style 462 Aero	TFP (800 tex (12 K)—(INR/INS))
Fabric type	Unidirectional	2/2 twill fabric	Unidirectional	2/2 twill fabric	TFP on Flaxply DB FAW 150
Grammage (g m^{-2})	110	150	230	250	12 k
Layer thinkness t (mm)	0.175	0.2	0.225	0.25	0.1
Fiber volume content V_F (%)	43	max. 41	50	50	–
Density (g cm^{-3})	1.183	1.257	1.518	1.42	1.5[a]
E_1 [GPa] (for wovens $E_1 = E_2$)	21.93	8.702	123.34	31.34	47.531
$E_2 = E_3$ [GPa] (for wovens E_3)	4.298	4.298	7.78	6.9	8.702
$V_{12} = V_{13}$ (for wovens V_{12})	0.38	0.23	0.27	0.4	0.27
V_{23} (for wovens $V_{23} = V_{13}$)	0.18	0.38	0.42	0.3	0.42[a]
$G_{12} = G_{13}$ [GPa] (for wovens G_{12})	1.5	16.23	5	19.5	5[a]
G_{23} [GPa] (for wovens $G_{23} = G_{13}$)	926	1.293	3.08	2.7	3.08[a]
$\sigma_1^{(+)}$ [MPa] (for wovens $\sigma_1^{(+)} = \sigma_2^{(+)}$)	215	103	1632	805	738
$\sigma_2^{(+)} = \sigma_3^{(+)}$ [MPa] (for wovens $\sigma_3^{(-)}$)	31	31	34	50	103.8
$\sigma_1^{(-)}$ [MPa] (for wovens $\sigma_1^{(-)} = \sigma_2^{(-)}$)	− 60	− 60[a]	− 704[a]	− 509[a]	− 704[a]
$\sigma_2^{(-)} = \sigma_3^{(-)}$ [MPa] (for wovens $\sigma_3^{(-)}$)	− 45	− 45[a]	− 68[a]	− 170[a]	− 68[a]
$\tau_{12} = \tau_{23}$ [MPa] (for wovens τ_{12})	32	24	80	125	80[a]
τ_{23} [MPa] (for wovens $\tau_{13} = \tau_{23}$)	22	22	55	65	55[a]
$\varepsilon_1^{(+)}$ [%] (for wovens $\varepsilon_1^{(+)} = \varepsilon_2^{(+)}$)	1.2	1.85	1.43	1.26	1.5
$\varepsilon_2^{(+)} = \varepsilon_3^{(+)}$ [%] (for wovens $\varepsilon_3^{(+)}$)	0.85	0.85	0.26	0.8	1.9[a]
$\varepsilon_1^{(-)}$ [%] (for wovens $\varepsilon_1^{(-)} = \varepsilon_2^{(-)}$)	− 1.5	− 1.5[a]	− 0.6[a]	− 1.02[a]	− 0.6[a]
$\varepsilon_2^{(-)} = \varepsilon_3^{(-)}$ [%] (for wovens $\varepsilon_3^{(-)}$)	− 2	− 2[a]	− 1.46[a]	− 1.2[a]	− 1.46[a]
$\varepsilon_{12} = \varepsilon_{13}$ [%] (for wovens ε_{12})	2.78	2.83	1.6	2.2	1.6[a]
ε_{23} [%] (for wovens $\varepsilon_{13} = \varepsilon_{23}$)	2.78[a]	2.78[a]	1.2	1.9	1.2[a]

[a]The characteristic values were taken from the technical data sheets or literature or assumed on the basis of empirical values

aero-dynamic load resulting from fast forward flight and an orthogonal wind gust of 10 m/s or 139 N/m^2 (Fig. 2).

The deformations resulting from the FEM simulation are shown in Fig. 3. This shows a maximum deformation of the bottom corner of 21.537 mm.

In actual operation, the cabin door is, therefore, lifted outward by approx. 21.5 mm due to the prevailing vacuum. This gap may no longer be bridged by the rubber seal, which means that the tightness of the booth can no longer be guaranteed. For this reason, a smaller permissible deformation of approx. 20 mm is defined as the target value for the design. The laminate weight and the calculated deformation or the resulting efforts are used as reference variables in the further course of the component optimisation.
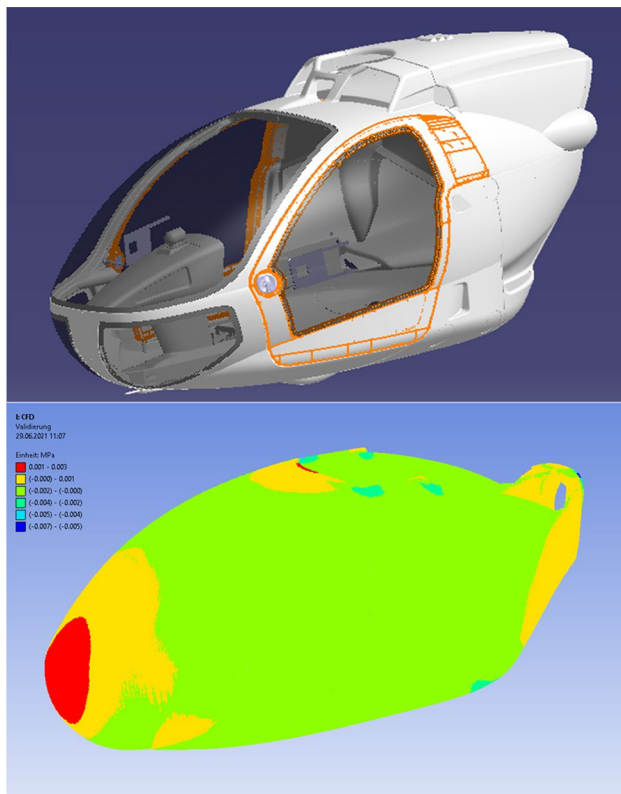
4.1 Definition of the TFP geometry

From the literature, some academic and commercial approaches for the derivation of the 2D or 3D TFP geometry are known. Software tools such as Abaqus Add-on CAIO (Computer-Aided Internal Optimization) [4], TACO (Tailored Composite Design Code) [11] or the EDOstructure (AOPS) [5] are particularly worth mentioning in this context. On the basis of various computational algorithms, corresponding principal stress lines are visualised automatically using principal stress integration and trajectories for the TFP geometry are derived in a further step. In this work, a new type of routine was developed for the design of the TFP geometry using the two available FE tools for the calculation and optimisation of fiber composites—Altair HyperWorks 2019 and Ansys Workbench 19.2 (Fig. 4). In addition, the CAD programs Solidworks and SpaceClaim were used to edit the geometry, and the Ansys Direct Optimisation plug-in was used for parametric FRP optimization.

The design routine essentially consists of 2 calculation steps. In the first step, Altair Hyperworks uses what is known as Topography Optimization (also referred to as Free Sizing Optimization) to determine the particularly stressed

Fig. 2 Cabin of the UHL CoAx2D (top, source: EDM Aerotec GmbH) and results of the CFD analysis (bottom)
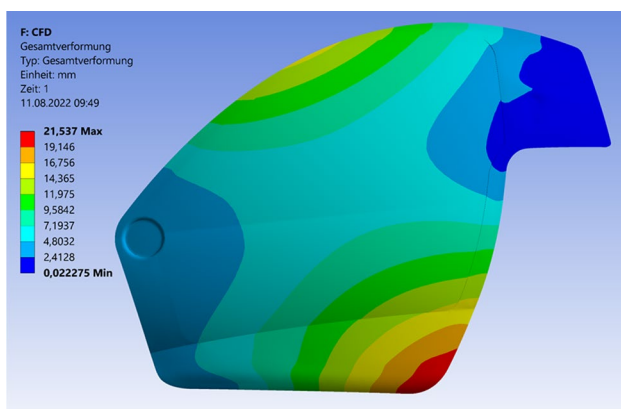
Fig. 3 Deformation plot of the reference door made of CFRP computed in Ansys Workbench 19.2

component areas and derive the TFP geometry. Free Sizing Optimization is commonly used to generate a thickness distribution for each defined fiber orientation and can be used to interpret the cutting geometry of the semi-finished products [12]. In this case, an analogous procedure is followed, using optimization results to define the TFP geometry and TFP direction.

At the beginning of the optimization, the FEM model for the outer and inner shells has a four-layer laminate structure $[0°; 45°; -45°; 90°]_{sym}$. The laminates are arranged symmetrically to each other. The base material is defined as FlaxPly 110 with a single layer thickness of 0.125 mm. This material has the highest mechanical properties compared to results of other investigated flax fiber semi-finished products [13]. The stack thickness is initially 1 mm (8 plies) per fiber direction. Topography optimization reduces the layer thicknesses until the specified convergence criterion is reached. In Fig. 5, the deformation at the beginning and at the end of the topography optimization is shown. Convergence after 56 iteration steps is reached at max. deformation of 19.76 mm.

Figure 6 illustrates the discrete thickness distribution of the stack depending on the fiber direction. The areas marked in light blue are locations that can only be modelled with a flax UD layer. The red areas indicate heavily stressed structural segments that need to be reinforced with an 8-layer UD laminate. In this case, the use of TFP reinforcement is appropriate. Based on the FE results and the lack of possibility to change the profile geometry of the circumferential door profile with the smallest cross section for the purpose of increasing the area moment of inertia, this area (Fig. 6, [90°] right) is modelled with TFP. Due to a rather diffuse principal stress distribution, the insertion of the CF fabric is preferable to the TFP reinforcement in the hinge area. Green–red area at 0° directions is implemented with 4 layers of CF-UD fabric.

The base laminate for the outer shell was a 4-ply $[0°; 45°; -45°; 90°]$ laminate developed from FlaxTape 110. Due to limited draping properties of FlaxTape 110, a 2-ply $[0°; 45°]$ laminate of flax fabric FlaxPly BD FAW 150 is used for the inside shell. The hinge areas of then cabin door are made of CF fabric with a $[0°; 45°]$ laminate. To improve the accuracy of the simulation results, the overlapping areas (20 mm) are also designed. The window was defined as a 4 mm thick shell of isotropic transparent PMMA (Plexiglas). In the design no core material was defined. In SolidWorks, the geometry for the TFP reinforcement is defined using the results shown in Fig. 6 for 90° direction and manually converted into an embroidery pattern. The laminate thickness distribution of the bio-based cabin door is shown in Fig. 7.

4.2 Optimization of the laminate

The Ansys plug-in "Direct Optimization" offers several methods for single and multi-objective optimization for FRP problems: Screening (based on sampling and sorting), NSGA-II-based generic algorithm, NSGA-II-based adaptive multi-objective method (restricted to continuous input parameters), nonlinear programming using quadratic Lagrangian (SQP, suitable for local refinement of single objectives with continuous parameters), mixed integer

Fig. 4 Developed routine for holistic design of hybrid natural fiber composites with TFP reinforcement
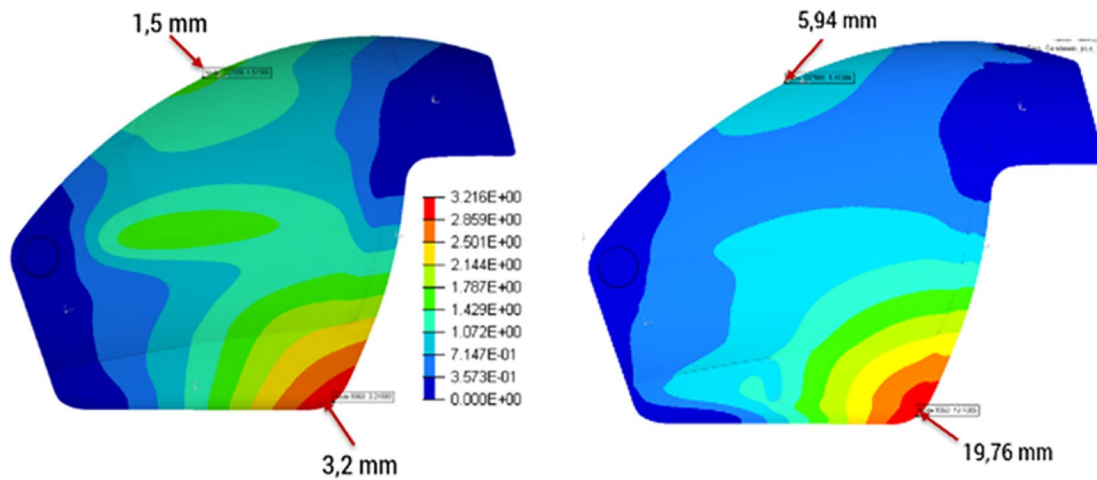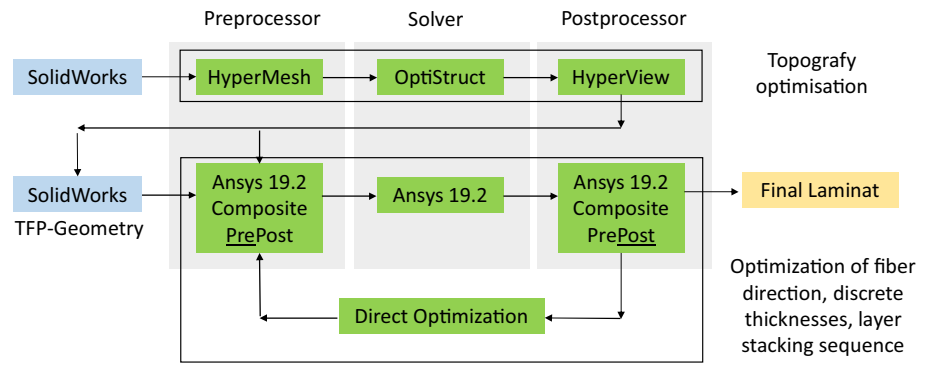
Fig. 5 Displacements in *z*-direction at the beginning (left) and at the end of the topography optimization (right) (shown with PMMA-window)
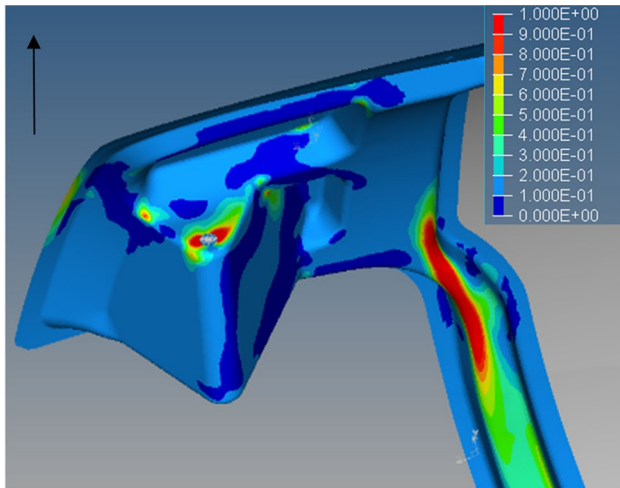

Fig. 6 Result of topography optimization for fiber directions in 90° (material thickness in mm)

sequential quadratic programming (MISQP), and gradient-based single objective method for continuous parameters

[14]. Multiple mutually conflicting objective functions can also be considered to find reasonable weighting factors for subsequent single-objective optimization and to develop a suitable design.

The fiber material, the fiber angle, the number of layers and the layer sequence can be defined as input variables for the optimization. For the objective functions, a choice can be made between component weight and deformation, local or global stresses and strains, or local or global failure. Due to the relatively simple laminate design with minimum laminate thickness, the input variables were limited to fiber direction and layer stacking order and, for the objective function, to part global deformation. MISQP was selected as the optimization method for its ability to solve mixed-integer nonlinear problems with a modified gradient-based single objective method for continuous parameters. Assuming that integer variables have a continuous influence on the model, sequences of quadratic approximations are applied. These support the computation of a single output parameter objective with multiple constraints [15].
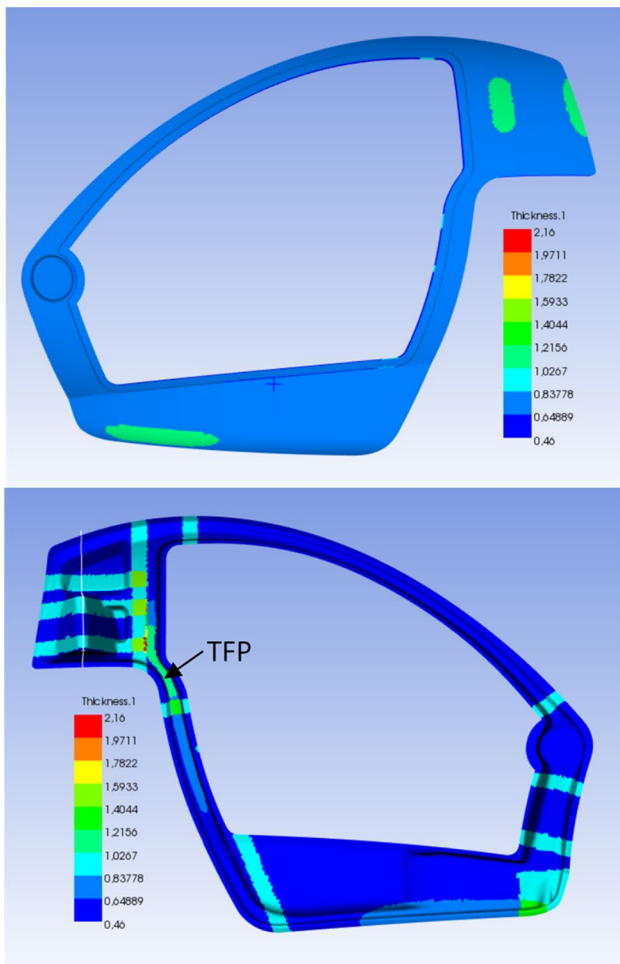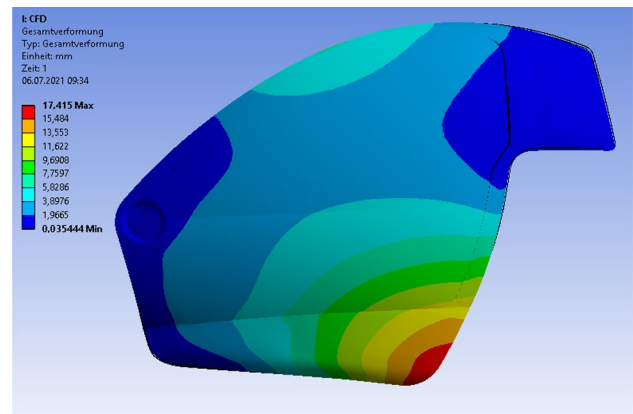
Fig. 7 Laminate thickness distribution of the outside (top) and inside (bottom) shell of the developed bio-based cabin door (shown without PMMA-window)
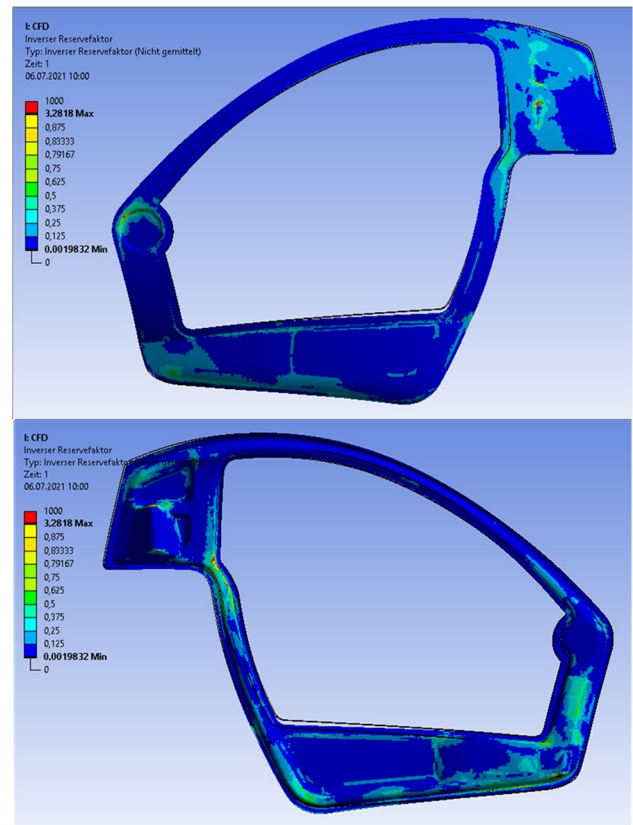

Fig. 8 Deformations the optimized bio-based cabin door (shown with PMMA-window)

The failure behaviour was analysed with the failure criterion according to PUCK 2D (Fig. 9) [16]. The puck constants were taken from CFRP, since no characteristic values could be determined for flax fiber composites yet. Table 2 illustrates the parameters used in the FE simulation for Puck's fracture criterion.

4.3 Results of the laminate design

During the design and optimization process, a preferred solution was developed with a basic laminate structure consisting of a FF UD (FlaxTape 110) or FF fabric (Flax-Ply BD 150) and partial reinforcements of CF TFP patches and CF scrim (Zoltek TMP PX35)/fabric (BD Style 462) in heavily loaded areas. In Fig. 8, the deformations of the CFRP and bio-based car doors are compared. With a deformation of 17.415 mm, the optimized door is stiffer by a factor of 1.24 (Fig. 9). The deformation pattern is also more homogeneous.

The calculated biomass fraction of the developed cabin door is only about 29 wt% due to the use of a 19 wt% bio-based resin component of the EP system, synthetic rigid foam inserts and structural adhesives. With a fully bio-based EP system and bio-based adhesives and sealants, a biomass content of more than 70 wt% could be achieved.

Fig. 9 Failure plots according to Puck's failure criterion (shown without PMMA-window)

Table 2 Parameters used in the FE simulation for Puck's fracture criterion

Parameter	Value
$p21(+)$	0.325
$p21(-)$	0.275
$p22(+)$	0.225
$p22(-)$	0.225
Reduction factor s $(0 < s < 1)$	0.5
Reduction factor M $(0 < M < 1)$	0.5
Interface weakening factor	0.8

Table 3 Multiples of the vibration frequencies of the rotor and engine (experimentally determined)

Component	Basic freq	2nd	3th	4th
Rotor	7.33	14.66	21.99	29.32
Engine	46.67	93.34	140.01	186.68
	5th	6th	7th	8th
Rotor	36.65	43.98	51.31	58.64
Engine	233.35	280.03	326.69	373.36

It has to be noted that the results are only of limited significance due to the assumed pressure-based characteristic values and correction factors. For example, lower puck constants and smaller compression-induced interfiber break spaces have been determined in [8] for comparable unidirectional flax fiber laminates. Nevertheless, the failure pattern, especially in the area of the narrowest circumferential cross section (enhanced by TFP patches), could be improved significantly. No convergence could be achieved for failure as an objective function for optimization. This was due to excessive local stresses in the area of the bearing.

In addition to mechanical stress due to (fluid) mechanical loads, the ULH is subject to high vibration stress. The improvement of the damping properties is among the main reasons for the use of flax fibers [13]. To illustrate this material advantage, an additional FE-based modal analysis was performed in this work. According to the specifications, resonances with 1 to 8 times the rotor and motor frequencies have to be eliminated for the cabin door (Table 3). A tolerance of $\pm 3\%$ applies in this case. In addition to avoiding resonances, low eigenfrequencies are also to be aimed at for acoustic reasons.

In the FE modal analysis, the basic frequencies of the first 20 modes were checked for resonance with the (multiple) rotor and motor frequencies. As soon as the basic frequency corresponded to $\pm 3\%$ of the excitation frequencies, resonance was assumed. For the CFRP cabin door, the eigenfrequencies occur at 5 modes and for the bio-based variant only at 3 modes (Table 4).

Table 4 Critical eigenfrequencies determined using FE simulation

Mode	CFRP Cabin door Frequency (Hz)	Mode	Bio-based cabin door Frequency (Hz)
2	47.441	1	45.438
4	91.292	4	91.387
9	139.73	12	139.67
10	143.84		
17	190.13		
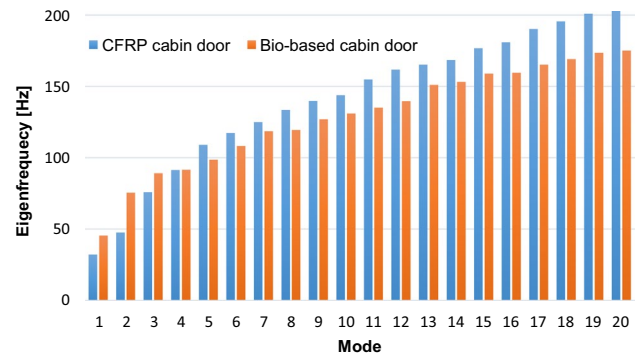
Fig. 10 Comparison of the eigenfrequencies of the CFRP and bio-based cabin door

Particularly in the higher modes, the damping properties of the flax fibers have a clear influence on the vibration behavior (see Fig. 10). Here, the basic frequencies are significantly below those of the reference cabin door made of CFRP. At this point, however, it has to be noted that the "soft" PMMA window contributes significantly to the vibration behavior and influences it more strongly than the fiber composite structure.

5 Validation of the FEM results

For the production of the bio-based cabin door, laminating molds were developed for the VARI or prepreg process and made from an Ebalta EP 978 foam material suitable for autoclave production. To reduce thermal stress during production, the molds are hollow on the inside. Due to the high infiltration resistance of flax fiber semi-finished products and the resulting slow flow front progress, a cascade-type infiltration system was made. The use of a Compolex 150 RF3 flow aid additionally accelerated the infiltration process. The cabin door was produced using the SuperSap INR/INS resin system in the aVARI process. The two half-shells were joined directly in the laminating mold using an adhesive Scotch Weld DP 490 2 K and specially made rigid foam inserts. The PMMA window pane was then inserted using a UV-resistant polyurethane hybrid sealant

Sikaflex 521. To prevent local failure at the hinge attachment a PVC foam core (80 g/mm^2) were bonded in the places of the hinges, which could minimally influence the measurement results. Figure 11 shows the completed bio-based cabin door. For demonstration purposes, the surface was partially painted.
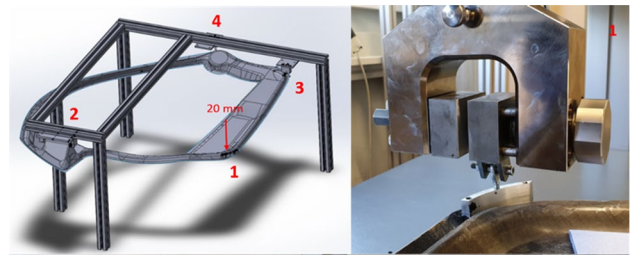
5.1 Mechanical testing of the cabin door

Based on the simulation results and design features, a realistic test setup (Fig. 12) was developed and simulated using FEM analysis. In real operation, the cabin door is supported in the helicopter cabin at three points, with all translational and rotational degrees of freedom in the x- and y-directions being locked at the hinge. When closed, the cabin door is locked at positions 3 and 4 in Fig. 12 by a manually operated locking mechanism (two locking bolts). Only the degree of translation along the bolt axis and the degree of rotational freedom are retained at the locking positions.

During the test, the lower corner of the cabin door (Position 1) was deflected via a bonded force application element and a hinge joint by means of a tensile/compression testing machine by 20 mm or 30 mm [corresponding to a safety factor (SF) of 1.5] in the z-direction. The resulting force was recorded with a load cell. The test was repeated 10 times in each case, an average value was calculated from the measurement results and compared with the calculated resultant force. During the test, the deformations at the stress-critical point with the smallest profile cross section (reinforced by TFP patches) were recorded three-dimensionally using an ARAMIS 3D optical deformation measurement system (Fig. 13). The measurement results have been used to verify the FE results.

Fig. 12 Test setup for testing the cabin door [1—force application, 2—hinge, 3—locking bolt (bottom), 4—locking bolt (centre)]

5.2 Results of the structural test

The force–displacement curve of the bio-based cabin door shows a reversible linear behaviour and a good agreement with the FE results (Table 5). With required deflection of the bottom corner of 20 mm, a mean force of 108.62 N results. Calculated value is 119 N, which is 10% higher than measured. Thus, at 20 mm deflection, the hybrid car door is only 10% more compliant than calculated, indicating good accuracy of the simulation.

Despite the less stiff behavior of the bio-based cabin door, an excellent qualitative and, above all, quantitative course of the displacements in the critical area (smallest profile cross section) can be observed (Fig. 14). The deviations from simulated values are between 7% and 12%. It can be concluded that the deformation of the cabin door is numerically well-represented and that the requirements have been met.

6 Summary and outlook

The design of the bio-based cabin door of the UHL CoAx2D was performed using a newly developed routine for deriving the TFP geometry with programs Hyperworks and Ansys

Fig. 11 Front side of bio-based cabin door (partially painted blue for demonstration purposes)

Fig. 13 Detection of surface displacements with an optical 3D measuring system ARAMIS

**Table 5** Results of component testing compared to FE results

	FEM	Experiment	Ratio
Reaction force at 20 mm traverse displacement (mm)	119	108.62	1.1
Reaction force at 20 mm traverse displacement (mm)	178.54	157.95	1.13
Displacement at 119 N (mm)	20.25	22.15	0.91

Workbench using a combination of free sizing, bundle sizing and shuffle optimisation. The primary optimisation objective variable was the deformation of the unattached lower car door corner of 20 mm, which is defined in the course of the aerodynamic load specified in the specifications and a wind gust of 10 m/s acting laterally outward. The FE results were validated by mechanical testing of the fabricated bio-based cabin door. For this purpose, a realistic test setup was developed and simulated based on the attachment and locking of the cabin door in the helicopter cabin. During component testing, the displacements of the component surface at

selected points were recorded using an optical 3D measuring system (Aramis) and compared with the FE results.

As a result, a compromise solution with a basic laminate structure consisting of a flax fiber scrim/fabric and partial reinforcements of CF TFP patches and CF scrim/fabric in heavily stressed areas was worked out after comprehensive material and technological consideration. With an actual weight of 985 g (without glued-in PMMA windows) and a biomass content of around 29 wt%, the hybrid bio-based cabin door is 255 g heavier than the reference variant made of CFRP. This is still within the permissible total weight defined in the specifications. In terms of ecological assessment, the use of bio-based raw materials can generate considerable added value, especially in the raw material and component manufacturing phase, but the associated increase in weight can lead to a higher CO_2 emission value in the long service life of the components. One conceivable approach to weight reduction is to use a lighter pre-impregnated flax fiber scrim (UD prepreg) instead of the "dry" semi-finished products. The high substitution potential of flax fibers and potentially achievable CO_2 savings compared to CFRP make the development of higher performance, fully bio-based semi-finished products a sensible and promising option.

Despite the added weight, the developed bio-based cabin door shows a better deformation and, according to FEM calculations, a damping behaviour at critical resonance frequencies in the range of 400–850 Hz that is about 30% more favourable. Furthermore, the measurement results confirm that topography optimization is well-suited for the design of TFP reinforcements with simple variable fiber design. In contrary, the downstream optimizations of the fiber direction, the discrete layer thicknesses as well as the stacking order of the base laminate structure did not improve the deformation behavior or the minimisation of the component weight any further. Considering the reasonable computational effort, this design methodology for developing of TFP reinforcements will be further pursued and optimised. Regarding the nonlinear, irreversible material behavior of UD flat fiber laminates under tensile/compressive loading as well as the fracture behavior of hybrid CF-FF laminates, numerous further essential questions remain to be addressed.
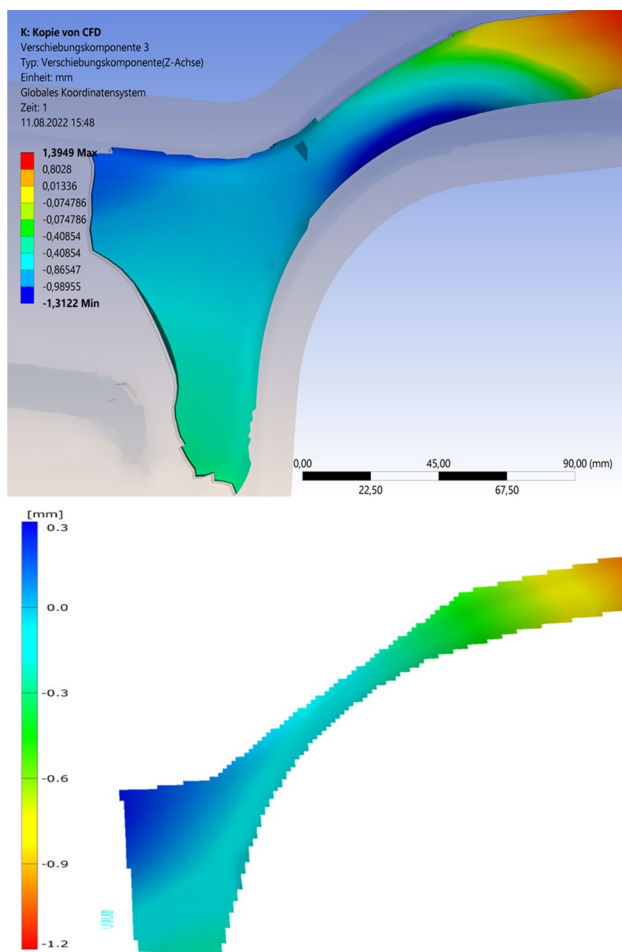
Fig. 14 Comparison of the measured (bottom—legend is sign-twisted) and simulated (top) displacements in the *z*-direction in the area of the smallest profile cross section at 20 mm deflection

References

1. Shehab, E., Meiirbekov, A., Amantayeva, A.: A cost modelling system for recycling carbon fiber-reinforced composites. Carbon Fiber Reinf. Compos. Polym. **13**, 4208 (2021). https://doi.org/10.3390/polym13234208

2. Uhlig, K., Bittrich, L., Spickenheuer, A.: Waviness and fiber volume content analysis in continuous carbon fiber reinforced plastics made by tailored fiber placement. Compos. Struct. **222**(15), 110910 (2019). https://doi.org/10.1016/j.compstruct.2019.110910

3. Fayazbakhsh, K., Nik, M.A., Pasini, D.: Defect leyer method to capture effect of gaps and overlaps in variable stiffness laminates made by Automated Fiber Placement. Compos. Struct. **97**, 245–251 (2013). https://doi.org/10.1016/j.compstruct.2012.10.031

4. Moldenhauer, H.: The orthotropic heat conduction as numerical integrator for general direction fields with application to tailored fiber placement and load path visualization. PhD-Thesis (2016). https://doi.org/10.5445/IR/1000060087

5. Spickenhauer, A.: Fiber reinforced plastics, part design, simulation, variableaxial, manufacturing, testing, tailored fiber placement, PhD-Thesis (2016). https://nbn-resolving.org/urn:nbn:de:bsz:14-qucosa-147748

6. Strohrmann, K., Andre, N., Hajek, M.: Hybrid natural fiber composites in a helicopter cabin door—mechanical properties and ecological efficiency. In: Presented at the VFS International 75th Annual Forum &Technology Display, Philadelphia, Indiana, USA, May 13–16, 2019. https://www.researchgate.net/publication/333581979_Hybrid_Natural_Fiber_Composites_in_a_Helicopter_Cabin_Door_-_Mechanical_Properties_and_Ecological_Efficiency

7. Strohrmann, K., Hajek, M.: Bilinear approach to tensile properties of flax composites in finite element analyses. J. Mater. Sci. (2018). https://doi.org/10.1007/s10853-018-2912-1

8. Koh, R., Madsen, B.: Strength failure criteria analysis for a flax fibre reinforced composite. Mech. Mater. **124**, 26–32 (2018). https://doi.org/10.3390/ma12060854

9. Koh, R., Madsen, B.: Strenght failure criteria analysis for a flax fibre reinforced composite. Mech. Mater. **124**, 26–32 (2019). https://doi.org/10.1016/j.mechmat.2018.05.005

10. Yan, L., Chouw, N., Jayaraman, K.: Flax fibre and ist composites—a review. Compos. Part B **56**, 296–317 (2014). https://doi.org/10.1016/j.compositesb.2013.08.014

11. Temmen, H., Degenhardt, R., Raible, T. Tailored fiber placment optimization tool. In: ICAS 2006—25th International Congress of the aeronautical Sciences (2006). https://www.icas.org/ICAS_ARCHIVE/ICAS2006/ABSTRACTS/590.HTM

12. Bromberger, M.: Strukturoptimierung in drei Schritten. MM Compositeworld **2014**, 24–27 (2014)

13. Schittkowsi, K. MISQP: A Fortran subroutine of a trust region SQP algorithm for mixed-integer nonlinear programming (2013). http://www.klaus-schittkowski.de

14. Rinberg, R., Svidler, R., Klärner, M., Kroll, L., Strohrmann, K., Hajek, M., and Endres, H.-J.: Anwendungspotenzial von naturbasierten hybriden Leichtbaustrukturen in der Luftfahrt. Deutscher Luft- und Raumfahrtkongress 2016 (2016). https://publikationen.dglr.de/

15. Barbero, E.J., Shahbazi, M.: Determination of material progressive damage analysis of laminated composites. Compos. Struct. **176**, 768–779 (2017). https://doi.org/10.1088/1757-899X/400/4/042031

16. Puck, A., Schürmann, H.: Failure analysis of FRP laminates by means of physically based phenomenological models. Special Issue of Comp. Sc. and Techn (1997)

17. Rueppel, M., Rion, J., Dransfeld, C., Masania, K.: Damping of carbon fibre and flax fibre reinforced angle ply polymers. In: ECCM 17—17th European Conference on Composite Materials (2016). https://doi.org/10.1016/j.compscitech.2017.04.011

18. Poilane, C., Gehring, F., Yang, H., Richard, F. About Nonlinear Behavior of Unidirectional Plant Fibre Composite. In: Fangueiro R., Rana S. (eds.) Advances in Natural Fibre Composites - Raw Materials, Processing and Analysis, pp. 69–79. Springer International Publishing AG (2018). https://doi.org/10.1007/978-3-319-64641-1